Journal of Nuclear Materials 122 & 123 (1984) 1459-1465
North-Holland, Amsterdam

THERMAL EFFECTS AND EROSION RATES FROM X-RAY ENERGY DEPOSITION IN ICF REACTOR FIRST WALLS

Ahmed M. HASSANEIN

Argonne National Laboratory, Fusion Power Program, 9700 South Cass Avenue, Argonne, Illinois 60439

The deposition of x-ray energy resulting from the microexplosion in an inertial confinement fusion reactor and the subsequent thermal response of candidate wall coating and structural materials is examined. Evaporation losses and resulting melt layer thicknesses for these materials exposed to a variety of different x-ray energies and spectra are calculated. Softer x-ray energy spectra absorbed very near the surface are found to cause more evaporation losses but less melting than harder spectra with the same energy content. Substantial differences in the thermal response exist among potential coating materials such as beryllium (low atomic number, low melting point) and molybdenum and tantalum (high atomic numbers, high melting points). It is found that beryllium can for a wide range of x-ray energy spectra expected in fusion reactors, resist vaporization losses and resulting melt layer and consequently prolong the lifetime of first walls more than molybdenum and tantalum.

1. INTRODUCTION

The most challenging engineering problems encountered in inertially confined fusion (ICF) reactors design are associated with the protection of cavity surface components from damage due to the different types of radiation, i.e., neutrons, target debris and x-rays released from the thermonuclear burn. Neutrons with 14 MeV in energy have a large mean free path compared to wall thickness and will pass through without despositing a significant amount of energy. Contrary to the neutrons, ion debris energy will be absorbed in the first few microns of an unprotected first wall. For x-rays, depending on the energy spectrum and on the wall material, the absorption of the energy in the wall will range from a few microns to a few millimeters. About 25% of the energy released is in the form of charged particles and x-rays. Larger fractions of the energy in x-rays and ion debris can be obtained by designing a target with high density-radius product.[1]

The partition of the energy between x-rays and target debris also depends on the target design as well as on the energy source driving the thermonuclear burn. The fraction of the energy contained in x-rays could be larger than that contained in the target debris.[2] Other situations in which most of the non-neutronic energy to the wall will be carried by x-rays is in ICF reactors utilizing gas protection.[3] In these reactors the cavity is filled with an inert gas to stop the target debris from reaching the wall and the energy is reradiated from the gas back to the wall as photon radiation.

The deposition of x-ray energy in a short distance in the metallic first walls and in very short time will result in very high surface temperatures which may cause melting and evaporation. The purpose of this study is to examine the thermal response and the resulting vaporization losses and melt zone thicknesses for different candidate coating and wall materials. The deposition of x-ray energy and the response of a stainless steel, as structural first wall material coated with beryllium for wide x-ray energy spectra, is analyzed. A comparison is made among the potential candidate coating materials such as beryllium (Be), molybdenum (Mo), and tantalum (Ta) for various x-ray energy contents and spectra.

2. SPECTRA AND WALL LOADING

Depending on the details of target design, constituents, and the driver beam, a wide range of x-ray spectra are possible from the fusion-target microexplosions. A commonly used spectrum for low energy photons is the Blackbody or Planckian spectrum,[4] which is used when radiation emission is specified by the temperature of the emitter. X-rays spectra from structured targets containing high atomic number materials are expected to have a Blackbody distribution. The blackbody temperature will depend on the yield, mass, and composition of the target.[5] Exact spectra can only be described in detail by using sophisticated computer codes such as LASNEX,[6] which is very expensive to run and not always available. In this study, x-rays having blackbody spectra with temperatures vary from 0.1 keV to 10 keV are assumed. These reasonably represent the expected spectra in fusion reactors.[7,8] The mathematical representation of the blackbody spectrum is given by

$$S(E) = \frac{15F}{\pi^4 KT}\left(\frac{U^3}{e^U-1}\right) \qquad J/keV\text{-}cm^2$$

where

U = E/KT

KT = characteristic energy, keV

F = total fluence or energy density, J/cm^2

The wall loading from source photons will occur at a time equal to the cavity radius divided by the speed of light. This is only true for a medium where the dielectric constant is independent of the frequency so that the propagation of all energies will be at the same velocity. The temporal shape of the source will then be the temporal shape of the loading pulse. The deposition time for x-ray energy spectrum also depends on the target design, cavity condition, and on the dynamics of the thermonuclear burn. Reasonable deposition times are assumed to be between 10 to 100 ns[8]. The deposition of x-rays into first wall materials will strongly depend on the energy spectrum of these x-rays. Soft x-rays deposit their energy within a few micrometers of the wall's surface, very rapidly heating a thin layer of the first wall to a higher temperature. Harder x-ray energy spectra penetrate at a relatively larger distance into the material, therefore heating a larger mass to a lower temperature. However, for thermonuclear yield with most of the energy carried by the charged particles, most of their energy will be deposited in the first few microns of an unprotected wall posing serious problems at the surface of the wall.[8]

3. CALCULATIONAL MODEL

Monte Carlo and other photon transport codes are used to calculate x-ray energy deposition for complex absorber geometries. However, practical problems in ICF reactor design have relatively simple geometries and somewhat less detailed analyses are appropriate. Exponential deposition profile with sufficiently detailed treatment of photon-material interaction cross sections is used in this analysis. A photon cross sections library developed by Hunter[9] based on the work of Biggs[10] has been incorporated into this study. A good agreement is found between this cross sections library and other cross section files such as ENDF/B especially in the energy ranges expected in ICF reactors.[11]

The first wall thermal response and the resulting vaporization losses and melt zone thicknesses that are presented in this paper are computed with the A*THERMAL computer code.[12] The code solves the heat conduction equation with temperature varying thermal properties, and uses the surface temperature to compute the evaporation rate. The surface temperature is determined by both the boundary condition as well as by the kinetics of the evaporation process. The correct boundary condition for this problem requires partitioning of the

incident energy into conduction, melting, and evaporation. Since the reactor cavity is assumed symmetrical and the incident x-ray energy is considered isotropically distributed all over the walls, no radiation losses from the surface is assumed. Moving boundary conditions are used to account for surface recession from evaporation and also for the solid-liquid interface. For a description of the solution methods and a review of the evaporation models see references 13 and 14. The code A*THERMAL is modified to handle different layers of materials, i.e., a coating and a base material. The phase change calculation is extended to include both layers. Evaporation is only assumed to proceed from the front surface of the coating material.

The general characteristics of first wall evaporation and melting from target x-rays can be identified without specifying a particular target design or a target yield. The analysis is done parametrically assuming an x-ray energy density of 10 J/cm^2 and a spherical cavity reactor with 5 meter radius. The radius determines the start of x-ray energy deposition time, i.e., at a time equal the radius divided by the velocity of light. Larger radius will have a small effect on the thermal response of the wall for constant energy density. This is because photon radiations travel with the velocity of light and will reach the wall in a very short time. On the contrary, for target debris, larger radii can substantially reduce vaporization losses and melting zone thickness. This is primarily because of the energy and the time scale over which they are emitted. To relate cavity dimensions to energy fluence, note that for a spherical cavity 5 meters in radius, 1 J/cm^2 corresponds to about 3.14 MJ of energy. The effect of higher energy densities and up to 30 J/cm^2 on beryllium and tantalum response is investigated later in the paper. The coolant temperature is assumed to be 300°C throughout this calculation.

4. BERYLLIUM COATING ON STAINLESS STEEL WALL

Among the engineering solutions to protect the first solid surface of ICF reactor chambers is the use of a thin metallic coating. Only in this scheme another solid material is used to protect the chamber structural wall. In this section, the x-ray energy deposition and thermal response of both beryllium as coating material and stainless steel as base structural material is analyzed. Figure 1 shows the deposition of 10 J/cm^2 of x-ray energy in a 1 mm Be coating on a 1 mm stainless steel wall for different blackbody temperatures. The deposition of other energy densities but with the same blackbody temperature will have the same spatial distribution with different magnitudes. For the softer spectrum of 0.1 keV blackbody temperature, all the energy is absorbed in the first few microns of beryllium. For the 1.0 keV temperature spectrum only 75% of the energy is absorbed in the 1 mm beryllium while the remaining 25% is absorbed in the first 100 microns of stainless steel. For the harder spectrum of 10 keV temperature only 4% of the energy is absorbed in beryllium and about 87% of the energy is absorbed in stainless steel, while the remaining 9% of the total energy escapes from stainless steel back surface. The large increase in the energy density for the different blackbody temperatures at the stainless steel surface is primarily because of the large photon absorption cross section. Figure 2 shows the percentage of the x-ray energy absorbed in beryllium for different coating thicknesses as a function of the blackbody temperature. Increasing beryllium thickness from 0.5 mm to 2.0 mm will only increase the energy abosrbed in beryllium from 60% to 85% for a 1.0 keV blackbody spectrum. To absorb all x-ray energy in beryllium for the 1.0 keV spectrum, about 10 mm thickness is needed.

The large increase in the energy deposition at the stainless steel surface will cause a large temperature increase and consequently a

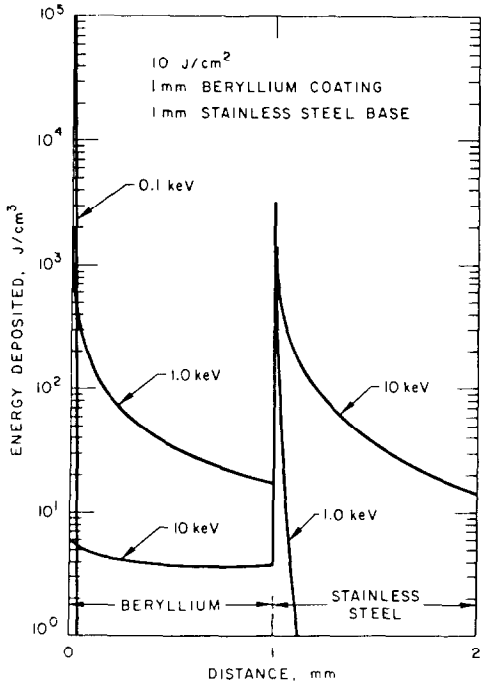

FIGURE 1
X-ray energy deposition in Be coating on stainless steel wall.

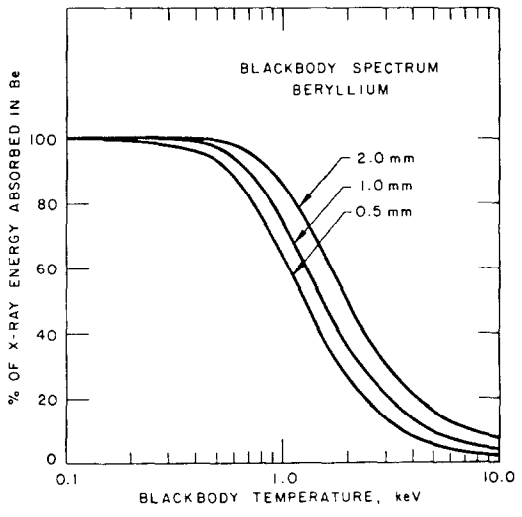

FIGURE 2
Percentage of x-ray energy absorbed in Be for different thicknesses and blackbody temperatures.

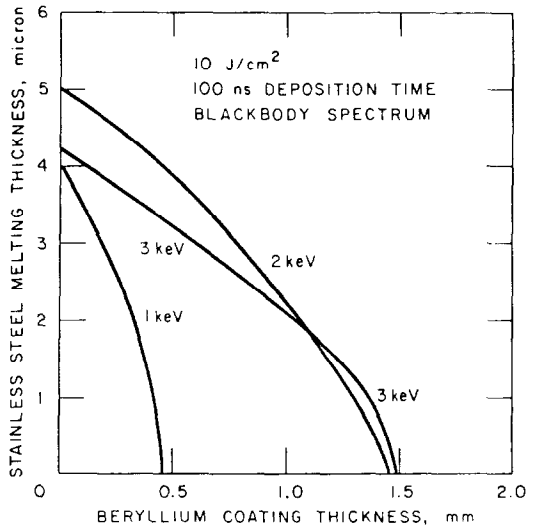

FIGURE 3
Stainless steel melting thickness for various thicknesses of Be coating.

melt layer can be formed. Figure 3 shows stainless steel melting thickness as a function of beryllium coating thickness for different blackbody temperatures. The x-ray pulse deposition time is assumed to be 100 ns. It can be seen that for a beryllium coating less than 1.5 mm thickness a melt layer on stainless steel surface up to 5 microns can be formed. For energy spectra with temperatures less than 1 keV most of the energy is deposited in beryllium coating (as shown in figure 2), and no melting zone will be formed in stainless steel. On the contrary, for energy spectra with temperatures larger than 3 keV, most of the energy is deposited in stainless steel but over larger volume leading to a smaller specific energy density which causes no melting. For the case where no beryllium coating is used, i.e., a bare stainless steel wall, in addition to the melt layer shown, a considerable amount of vaporization will occur.[3] It should be mentioned that in all the cases where stainless steel surface is melted, a small fraction less than a micron of the back surface of beryllium coating is also melted.

5. COMPARISON OF DIFFERENT COATING MATERIALS

In this section, a comparison is made in the response to x-ray energy deposition between the high melting point refractory metals, molybdenum and tantalum, and the relatively low melting point beryllium as major potential coating candidates for ICF reactors. Figure 4 shows the resulting melt layer thickness from a deposition of 10 J/cm^2 in 10 ns pulse duration for the three materials. It can be seen that for soft spectra with temperatures of 0.4 keV or less, beryllium melts more than tantalum or molybdenum. On the other hand, as will be shown later, beryllium shows the lowest vaporization losses among these materials for the same conditions. Figure 4 also shows that for spectra greater than 0.5 keV in temperature, beryllium does not melt, whereas molybdenum and tantalum continue to have a melt layer up to spectra with temperatures of 4.0 keV and 7.0 keV, respectively. The maximum melt layer for beryllium occurs around a blackbody temperature of 0.2 keV while it occurs around 1.5 keV and 2.5 keV for molybdenum and tantalum, respectively. The existence of a maximum is explained by the fact that for very soft spectra most of the energy goes to vaporization, leaving a smaller fraction of the energy to be conducted and cause melting. For harder spectra the deposition is spread over a large mass of the material leading to a low specific energy density which tends to reduce both melting and vaporization. The amount of material vaporized for different blackbody temperatures is shown in Figure 5. The maximum vaporization loss occurs at the lowest x-ray energy temperature and decreases sharply as the temperature increases. Beryllium has the lowest vaporization loss compared to tantalum and molybdenum. Beryllium shows no significant vaporization loss for 0.5 keV temperature and larger, whereas molybdenum and tantalum show significant vaporization losses up to temperatures around 2 keV and 3 keV, respectively.

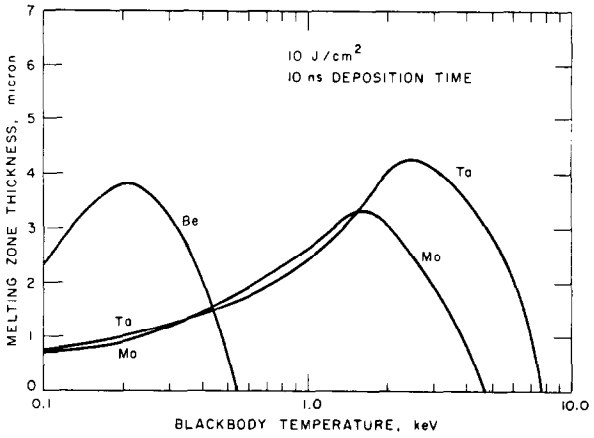

FIGURE 4
Melting zone thickness as a function of blackbody temperature.

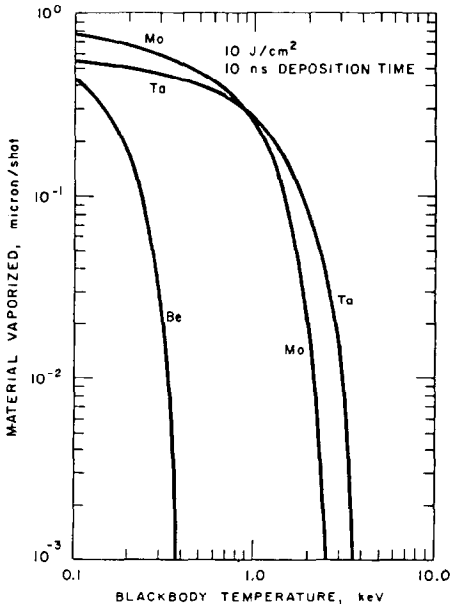

FIGURE 5
Vaporization losses as a function of blackbody temperature.

The effect of different x-ray pulse deposition times on the melt layer thickness of tantalum is shown in Figure 6. Longer deposition

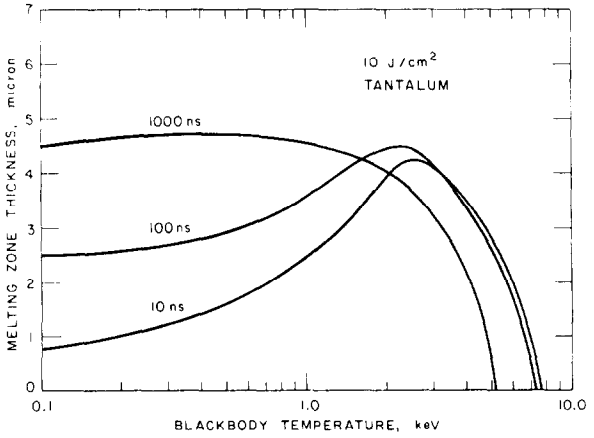

FIGURE 6
Ta melting zone thickness for different x-ray times.

times which allow more heat conduction into the material result in lower surface temperatures. This generally has the effect of reducing surface vaporization and increasing melt zone thickness as shown in Figure 6.

The effect of different x-ray energy densities on the vaporization and melting of beryllium and tantalum is illustrated in Figure 7. Energy densities up to 30 J/cm^2 (about 94 MJ of x-rays emitted in a spherical reactor of 5 m radius) with blackbody temperature of 0.5 keV, deposited in 100 ns are considered. This relatively soft spectrum can be absorbed in a 2 mm beryllium thickness (Figure 2), whereas about 10 microns of tantalum is sufficient to absorb this spectrum. Figure 7 shows that for energy densities up to 16 J/cm^2 (about 50 MJ incident on a 5 m radius reactor), no significant vaporization from beryllium occurs. On the other hand, considerable vaporization losses occur from tantalum for energy densities of 4 J/cm^2 or more. Below 8 J/cm^2, beryllium does not melt whereas melting occurs in tantalum for energy densities around 2 J/cm^2. For x-ray spectrum of 1.0 keV, beryllium does not show any melting or vaporization up to 30 J/cm^2, while tantalum

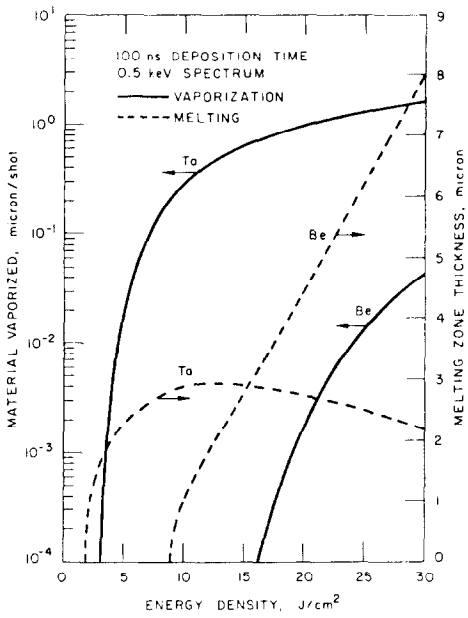

FIGURE 7
Vaporization losses and melting zone thickness as a function of energy density.

shows about 30% more melting and about 20% less vaporization. If the melt layer is assumed to be stable,[15] the erosion rate must not exceed a few angstroms per shot for a first wall lifetime to be on the order of the reactor lifetime. It appears for the x-ray energies and conditions studied here that beryllium can provide more protection and hence prolong the lifetime of an ICF reactor more than tantalum or molybdenum.

6. CONCLUSIONS

The parametric study of the first wall evaporation and melting from x-ray energy deposition shows that a thin metallic coating can protect a bare wall from erosion losses. Low atomic number materials such as beryllium filter out the low temperature components of the spectrum and spread the energy deposited over a larger volume leading to a lower specific energy density which has the effect of reducing melting and vaporization. Depending on the x-ray energy, spec-

trum, and deposition time, a few millimeters of beryllium could be enough to protect the wall structural material from severe temperature effects. For x-ray conditions studied in this paper, beryllium as coating material is much more effective than the refractory metals molybdenum and tantalum in protecting the first wall from erosion losses and can extend the wall lifetime by orders of magnitude longer. If the x-ray energy content and spectrum could be somewhat controlled by a specific target design, then releasing most of the non-neutronic energy in x-rays can lead to an easier protection of the first wall and longer lifetime than if most of this energy is to be carried away by the charged particles.

ACKNOWLEDGEMENTS

This work has been partially supported by the Department of Energy.

REFERENCES

1. J. A. Blink, P. E. Walker, and H. W. Meldner, Energy partition and neutron spectra from laser fusion reactor targets, in: Trans. ANS 1977 Winter Meeting, San Francisco, CA (1977) 70.

2. B. Badger, et al., HIBALL - A conceptual heavy ion beam driven fusion reactor study, in: University of Wisconsin Report UWFDM-450 and Karlsruhe Nuclear Laboratory Report, KfK-3202 (1981).

3. A. M. Hassanein, T. J. McCarville, and G. L. Kulcinski, J. Nucl. Mater. 103/104 (1981) 327.

4. Handbook of Physics; E. U. Condon and H. Odishaw, Editors; 2nd Ed. McGraw-Hill, (1967) pp. 7-26.

5. T. G. Frank, et al., Heat transfer problems associated with laser fusion, AICHE Symposium Series 73, No. 168 (1976) p. 77.

6. G. B. Zimmerman, Numerical simulation of the high density approach to laser-fusion, Lawrence Livermore Laboratory Report UCRL-74811 (October, 1973).

7. E. Sucov, et al., The Westinghouse ICF power plant study, WFPS-TME-80-014, (October 1980).

8. A. M. Hassanein, C. D. Croessman, and G. L. Kulcinski, Accepted for publication (Nuclear Technology/Fusion, 1983).

9. T. O. Hunter, A general model for the analysis of the transient radiation damage environment from pulsed thermonuclear radiation, Ph.D thesis, University of Wisconsin, (July 1978).

10. F. Biggs and R. Lighthill, Analytical approximations for total and energy absorption cross sections for photon-atom scattering, SC-PR-720685, Sandia Laboratories, Albuquerque, NM, (December 1972).

11. G. L. Simmons, J. H. Hubbell, Comparison of photon interaction cross section data sets II, Biggs-Lighthill and ENDF/B; NBS-10818, National Burreau of Standards, Washington, D.C., (March, 1972).

12. A. M. Hassanein, Ph.D Thesis, University of Wisconsin Report UWFDM-465 (1982).

13. A. M. Hassanein, G. L. Kulcinski, and W. G. Wolfer, J. Nucl. Mater. 103/104 (1981) 321.

14. A. M. Hassanein, G. L. Kulcinski, and W. G. Wolfer, to be published in Nuclear Engineering and Design/Fusion (1983).

15. W. G. Wolfer and A. M. Hassanein, J. Nucl. Mater. 111/112 (1982) 560.